EXPERIMENTS ON FLOW SEPARATION AT THE INNER BANK OF OPEN-CHANNEL BENDS

KOEN BLANCKAERT[1,2], MIAO WEI[1,2], JORIS HEYMAN[3], DANXUN LI[2] & ANTON J. SCHLEISS[1]

[1] *Laboratory of Hydraulic Constructions, ENAC, EPFL, Lausanne, Switzerland,*
koen.blanckaert@epfl.ch, anton.schleiss@epfl.ch

[2] *State Key Laboratory of Hydroscience and Engineering, Tsinghua University, Beijing, China,*
miaowei12358@126.com, lidx@mail.tsinghua.edu.cn

[3] *Environmental Hydraulics Laboratory, ENAC, EPFL, Lausanne, Switzerland,*
joris.heyman@epfl.ch

ABSTRACT

In spite of its hydraulic and morphologic importance, the conditions of occurrence of flow separation at the inner bank of open channel bends are still not known. In a series of 23 experiments in a laboratory open channel bend with flat sand bed, it was investigated how the process of inner-bank flow separation depends on two control parameters: the ratio of flow depth *H* to minimum radius of curvature *R*, and the Froude number *Fr*. The Froude numbers investigated were 0.1, 0.2, 0.3, 0.4 and 0.5 and the *H/R* values investigated were 0.038, 0.053, 0.077, 0.112 and 0.153. All flow conditions concerned strongly curved subcritical flow. Flow did separate from the inner bank in all experiments, but recirculation zones with reversed velocities did not develop. Surprisingly, the flow separation did not show any dependence on *Fr*. The point of flow separation moved farther downstream in the bend with increasing *H/R*.

Keywords: flow separation, curved flow, experiments, Froude number, curvature

1. INTRODUCTION

Flow separation at the inner bank has been observed in natural open-channel bends by e.g. Bagnold (1960), Leeder & Bridge (1975), Ferguson et al. (2003), Frothingham & Rhoads (2003), Nanson (2010), Schnauder & Sukhodolov (2012), and Rhoads & Massey (2012). Flow separation has broad and significant morphologic consequences. It favours the development of a deposition bar and the accretion of the inner bank. This can decrease the effective channel width and thus reduce the channel conveyance capacity, which can alter patterns of bed and bank erosion (Ferguson et al. 2003, Kleinhans et al. 2009).

In spite of its hydraulic and morphological importance, the process of flow separation remains largely unknown. According to Leopold et al. (1960), flow separation is best expressed as a function of Froude number *Fr* and bend tightness. Bagnold (1960), on the contrary, rejected the use of the Froude number because separation in pipes is similar to separation in open-channel flows, but *Fr* can only be defined in the latter. The bend tightness is commonly parameterized by means of the ratio *B/R*, where *B* is the channel width and *R* is the minimum radius of curvature (e.g. Hickin 1974, Hooke 2003). This ratio tends to zero for straight rivers, and reaches values higher than 1 for the sharpest bends occurring in nature (see compilation of field data in Crosato 2008). Flow separation at the inner bank only occurs in sufficiently sharply curved bends, but no clear quantitative criterion exists yet for the bend sharpness required for the onset of flow separation. Based on 23 field observations and measurements in four different bends in intertidal meandering channels, Leeder & Bridges (1975) have proposed a discriminative curve for the onset of flow separation as a function of *B/R* and *Fr*, with *Fr* in the range of 0.1 to 0.5 and *B/R* in the range 0.1 to 1. According to this curve, flow separation is favoured in tight bends and in flows with high *Fr*. This limited number of observations and measurements obviously can only give indications on the conditions required for the onset of flow separation.

The objective of the present paper is to examine the process and characteristics of inner-bank flow separation in open-channel bends as a function of bend tightness and *Fr* by means of detailed experiments in a laboratory flume.

2. THE EXPERIMENTS

Measurements were performed in a 1.3 m wide open-channel laboratory flume, including a bend with an arc length of 193° and a constant radius of curvature of 1.7 m on the centreline. The bend was preceded by a 9 m long straight inflow reach, and followed by a 5 m long straight outflow reach. The bed consisted of quasi-uniform sand with a diameter of 0.002 m. the bed was transversally flat, but had a longitudinal slope of 0.003. Flow depth was controlled with an adjustable weir at the downstream end of the flume. Because the longitudinal water surface slope was not equal to the longitudinal bed slope in all experiments, flow depth slightly and gradually varied along the flume, resulting in quasi-uniform flow conditions.

The geometric curvature in an open-channel bend depends on the centreline radius of curvature, *R*, the width of the flow, *B*, and the depth of the flow, *H*, which can be combined into two independent dimensionless parameters, such as *H/R* and *B/R*. In natural streams *R*, *B* and *H* are correlated according to Leopold *et al.* (1960) and curvature can therefore be parameterized by one of the dimensionless parameters. Field studies typically make use of the dimensionless curvature ratio *B/R*. In laboratory studies, *R* and *B* are fixed by the flume geometry, whereas it is straightforward to modify *H*.

Therefore, the present study adopts *H/R* to parameterized bend tightness. Experiments were performed at flow depths of *H* = 0.065 m, 0.09 m, 0.13 m, 0,19 m, and 0.26 m, corresponding to curvature ratios of *H/R* = 0.038, 0.053, 0.077, 0.112 and 0.153, which range from moderately curved to very strongly curved flows. These flow depths were measured at the centreline in the cross-section at 75° in the bend. For each of these flow depths, experiments were performed at *Fr* = 0.1, 0.2, 0.3, 0.4, and 0.5. Because of limited pump capacity, experiments at *Fr* = 0.4 and 0.5 were not possible for the highest flow depth.

Velocity patterns at the water surface were measured by means of digital videography of neutrally buoyant particles with a diameter of about 0.001 m that floated at the water surface. Particle images were captured at a sampling rate of 33 frames per second with a high speed, 1280 x 1024 pixel^2 CMOS camera (SMX-155, monochrome). A 12 mm wide-angle lens was used to maximize measuring area and minimize distortion error. A LED light provided sufficient illumination to reduce image streaking. The camera was positioned at a fixed distance above the channel bed, implying that the spatial resolution varied (7.0 pixel/cm to 10.0 pixel/cm) with the water depth. By moving the camera along the channel, the entire area of interest could be covered. For each test, a total number of 900 frames were gathered for calculating surface velocity. Tracer particles were tracked by using the match probability method (Li et al., 2012).

3. RESULTS, DISCUSSION AND CONCLUSIONS

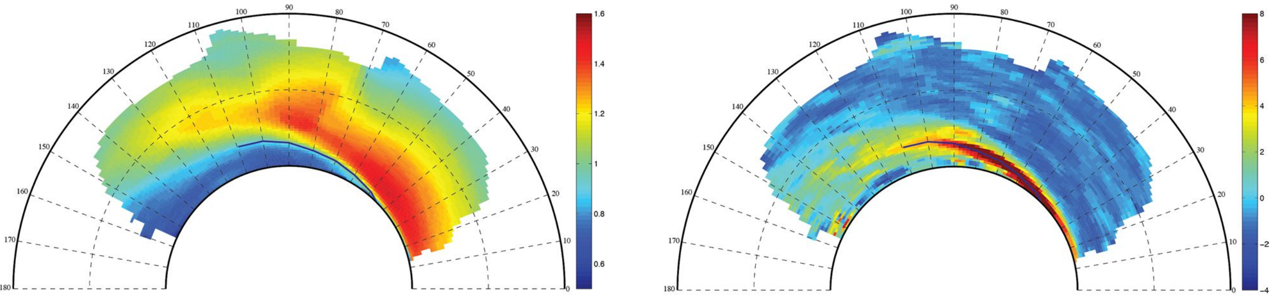

Figure 1: Experiment with flow depth of 0.13 m in the cross-section at 75 ° in the bend and *Fr* = 0.1. Flow is from right to left. (left) Pattern of normalized streamwise velocity at the surface, $v_{s,surf}/U$; (right) Normalized transverse gradient of the surface velocity, $(\partial v_{s,surf}/\partial n)/(U/R)$.

The left panel in Figure 1 shows the resulting velocity pattern at the water surface in the experiment with *H* = 0.13 m and *Fr* = 0.1. Flow separates from the inner bank at about 45° in the bend. A shear layer separates the fastest moving main flow from the considerably slower moving flow in the zone of inner-bank flow separation. Velocities in the separation zone are small, but remain downstream oriented, i.e. no flow recirculation vortex develops in the zone of inner-bank flow separation. The shear layer at the edge of the zone of inner-bank flow separation is even better discernable in the pattern of the transverse gradient of the streamwise velocity at the surface. The right panel in Figure 1 shows that the shear layer coincides with maximum values of this quantity.

Figure 2 summarizes the results of all 23 experiments. The figure indicates the position of the edge of the zone of inner-bank flow separation for each of the investigated flow depths, and for each of the *Fr* numbers. These results lead to the following conclusions.

First, flow separation did occur for all investigated experiments. This results is surprising, because flow separation was not expected to occur in the experiments with the lowest Froude numbers and moderate curvature of the streamlines, corresponding to the lowest flow depths.

Second, the process of inner-bank flow separation was found to be independent of the Froude number. This is again an unexpected result, because the discriminative curve proposed by Leeder and Bridges (1975) identified *Fr* as one of the dominant control parameters.

Third, the flow separates farther downstream in the bend with increasing values of *H* and *H/R*. Moreover, the zone of inner-bank flow separation becomes wider and persists over a longer streamwise distance.

ACKNOWLEDGMENTS

The research was funded by the Sino-Swiss Science and Technology Cooperation, Institutional Partnership, grant numbers IP13_092011 and FU07-0302014.

REFERENCES

Bagnold R.A. (1960). Some aspects of the shape of river meanders. *U.S. Geological Survey Professional Paper 282-E*, U.S. Geological Survey, Washington, D.C.

Crosato A. (2008). Analysis and modelling of river meandering. Ph.D. dissertation, Delft Univ. of Technol., Delft, Netherlands.

Ferguson R.I., Parsons D.R., Lane S.N., and Hardy R.J. (2003). Flow in meander bends with recirculation at the inner bank. *Water Resour. Res.,* 39(11), 1322-1333.

Frothingham K.M., and Rhoads B.L. (2003). Three-dimensional flow structure and channel change in an asymmetrical compound meander loop, Embarras River, Illinois. *Earth Surf. Processes and Landforms,* 28(6), 625-644.

Hickin E.J. (1974). The development of meanders in natural riverchannels. *Am. J. Sci.,* 274, 414–442.

Hooke J. (2003). River meander behaviour and instability: A framework for analyses. *Trans. Inst. Br. Geogr.,* 28(2), 238–253.

Kleinhans M.G., Schuurman F., Bakx W., and Markies H. (2009). Meandering channel dynamics in highly cohesive sediment on an intertidal mud flat in the Westerschelde estuary, The Netherlands. *Geomorphology,* 105, 261-276.

Leeder M.R., and Bridges P.H. (1975). Flow separation in meander bends. *Nature*, 253(5490), 338-339.

Leopolod L.B., Bagnold R.A., Wolman M.G., and Brush L.M. (1960). Flow resistance in sinuous or irregular channels. *U.S. Geological Survey Professional Paper 282-E*, U.S. Geological Survey, Washington, D.C.

Li D., Qu Z., Yu M., Wang D., and Wang X. (2012). Particle Tracking Velocimetry: principles and applications. *Science Press*, Beijing (in Chinese).

Nanson R.A. (2010). Flow fields in tightly curving meander bends of low width-depth ratio. *Earth Surf. Processes and Landforms*, 35(2), 119–135.

Rhoads B.L., and Massey K. (2012). Flow structure and channel change in a sinuous grass-lined stream within an agricultural drainage ditch: implications for ditch stability and aquatic habitat. *River Research and Applications*, 28(1), 39-52.

Schnauder I., and Sukhodolov, A.N. (2012). Flow in a tightly curving meander bend: Effects of seasonal changes in aquatic macrophyte cover. *Earth Surf. Processes and Landforms*, 37(11), 1142–1157.

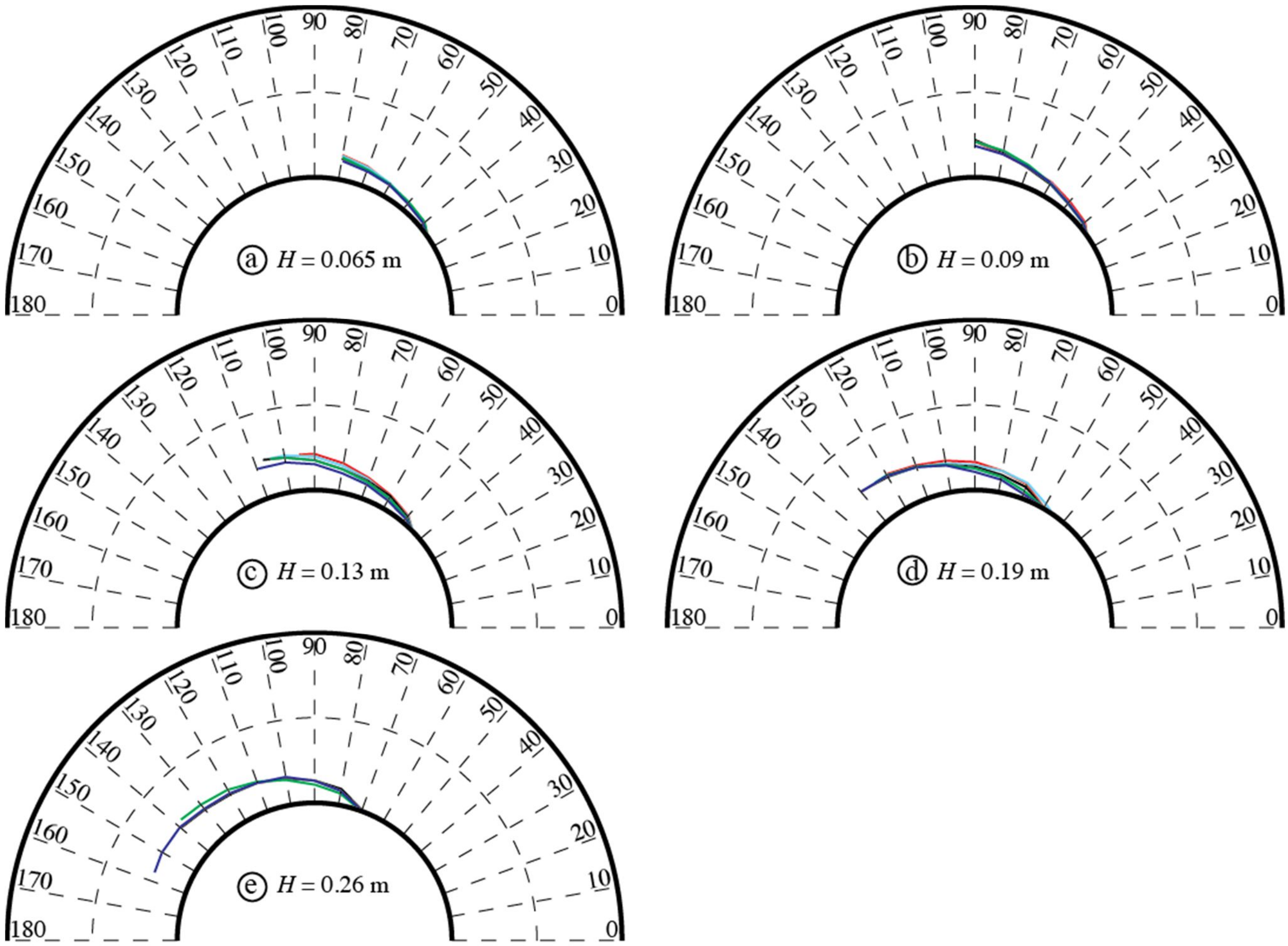

Figure 2. Shear layer at the edge of the zone of inner-bank flow separation. The flow depth at 75 ° in the curved reach is indicated in each figure. The Froude number is indicated by colors: Fr = 0.1 (blue), Fr = 0.2 (green), Fr = 0.3 (black), Fr = 0.4 (cyan), Fr = 0.5 (mauve).